Interplay between the tyrosine kinases Chk, Csk and phosphatase PTPRJ is critical for regulating platelets in mice.

Nagy, Zoltan; Mori, Jun; Ivanova, Vanesa-Sindi; Senis, Yotis

Interplay between the tyrosine kinases Chk, Csk and phosphatase PTPRJ is critical for regulating platelets in mice

Short title: Chk, Csk and PTPRJ: critical platelet regulators

Zoltan Nagy,[1,2*] Jun Mori,[1*] Vanesa-Sindi Ivanova,[1] Alexandra Mazharian,[1,3] and Yotis A. Senis,[1,3]

[1]Institute of Cardiovascular Sciences, College of Medical and Dental Sciences, University of Birmingham, Birmingham, UK
[2]Institute of Experimental Biomedicine, University Hospital Würzburg, Würzburg, Germany
[3]Université de Strasbourg, Institut National de la Santé et de la Recherche Médicale, Etablissement Français du Sang Grand Est, Unité Mixte de Recherche-S 1255, Fédération de Médecine Translationnelle de Strasbourg, Strasbourg, France
[*]Z.N. and J.M. contributed equally to this study

Correspondence:
Yotis A. Senis
Université de Strasbourg, Institut National de la Santé et de la Recherche Médicale, Etablissement Français du Sang Grand Est, Unité Mixte de Recherche-S 1255, Fédération de Médecine Translationnelle de Strasbourg, Strasbourg, France; email: yotis.senis@efs.sante.fr

Word count for text: 4,000
Word count for abstract: 249
Figure/table count: 7 figures, 1 supplemental table
Reference count: 55

Key points

Chk, Csk and PTPRJ are the main regulators of SFKs in platelets, which play a key role in maintaining platelet count.

SFKs are able to auto-regulate their activity by phosphorylating either their activation loop or C-terminal inhibitory tyrosine residue.

Abstract

The Src family kinases (SFKs) Src, Lyn and Fyn are essential for platelet activation and also involved in megakaryocyte (MK) development and platelet production. Platelet SFKs are inhibited by C-terminal Src kinase (Csk), which phosphorylates a conserved tyrosine in their C-terminal tail, and are activated by the receptor-type tyrosine phosphatase PTPRJ (CD148, DEP-1), which dephosphorylates the same residue. Deletion of Csk and PTPRJ in the MK lineage in mice results in increased SFK activity, but paradoxically hypoactive platelets due to negative feedback mechanisms, including upregulation of Csk homologous kinase (Chk) expression. Here, we investigate the role of Chk in platelets, functional redundancy with Csk and the physiological consequences of ablating Chk, Csk and PTPRJ in mice. Platelet count was normal in *Chk* knockout (KO) mice, reduced by 92% in *Chk;Csk* double KO (DKO) mice, and partially rescued in *Chk;Csk;Ptprj* triple KO (TKO) mice. Megakaryocyte numbers were significantly increased in both DKO and TKO mice. Phosphorylation of the inhibitory tyrosine of SFKs was almost completely abolished in DKO platelets, which was partially rescued in Src and Fyn in TKO platelets. This residual phosphorylation was abolished by Src inhibitors, revealing an unexpected mechanism in which SFKs auto-inhibit their activity by phosphorylating their C-terminal tyrosine residues. We demonstrate that reduced inhibitory phosphorylation of SFKs leads to thrombocytopenia with Csk being the dominant inhibitor in platelets, and Chk having an auxiliary role. PTPRJ deletion in addition to Chk and Csk ameliorates the extent of thrombocytopenia, suggesting targeting it may have therapeutic benefits in such conditions.

Introduction

Src family kinases (SFKs) are essential for initiating and propagating activation signals from a variety of platelet receptors, including the immunoreceptor tyrosine-based activation motif (ITAM)-containing collagen receptor complex GPVI-FcR γ-chain and the fibrinogen receptor integrin αIIbβ3.[1] SFKs also initiate inhibitory signaling from immunoreceptor tyrosine-based inhibitory motif (ITIM)-containing receptors, including the megakaryocyte and platelet inhibitory receptor G6b-B (MPIG6B) and platelet endothelial cell adhesion molecule (PECAM-1).[2,3] In platelets, SFKs are regulated by C-terminal Src kinase (Csk), which phosphorylates a conserved tyrosine residue in the C-terminal tail of SFKs, restraining them in an inactive conformation; and by the receptor-type tyrosine phosphatase PTPRJ (CD148, DEP-1, RPTPη), which dephosphorylates the same tyrosine residue, thereby releasing SFKs from their auto-inhibited conformation.[2,4-6] *Trans*-auto-phosphorylation of a conserved tyrosine residue in their activation loop stabilizes the active conformation. PTPRJ is also able to attenuate SFK activity by dephosphorylating the activation loop tyrosine.[2,6-8] Targeted deletion of *Csk* and *Ptprj* in the megakaryocyte (MK) lineage of mice results in significantly elevated SFK activity, but paradoxical hypo-active platelets, reduced thrombosis and increased bleeding, due to negative feedback pathways, including downregulation of GPVI-FcR γ-chain and the hemi-ITAM-containing podoplanin receptor CLEC-2, and concomitant upregulation and phosphorylation of the inhibitory receptor MPIG6B.[2]

Src and Lyn also play important roles in MK development and platelet production as exemplified by human and mouse genetic studies. The gain-of-function mutation in human *Src* (E527K), resulting in loss of Src auto-inhibition, causes thrombocytopenia and a reduction in proplatelet formation.[9,10] Moreover, *Lyn* knockout (KO) mice display increased MK progenitor cell proliferation and a greater number of mature MKs with increased ploidy *in vitro* and more MKs in the bone marrow.[11-13] Although, *Lyn* KO and *Src* KO mice do not display

major differences in platelet count compared to control mice due to the overlapping roles of these SFKs, mice deficient in both *Lyn* and *Src* develop thrombocytopenia.[14] The critical role of Src and Lyn in MK maturation and proplatelet formation is further consolidated by tyrosine kinase inhibitor studies. Pharmacological inhibition of SFKs by PP1, PP2, SU6656 or dasatinib results in enhanced proliferation and maturation of cultured megakaryocytes,[11,15,16] and increased platelet production of inhibitor-treated MKs infused to mice *in vivo*.[17]

The two main regulators of platelet SFKs, namely Csk and PTPRJ, also play key roles in MK function and platelet production. *Pf4-Cre*-generated *Csk* KO mice display a 65% reduction in platelet count, whereas *Gp1ba-Cre*-generated *Csk* KO mice, in which recombination occurs later in MK development, show a 32% decrease in platelet count, highlighting a key role of Csk in MK development and platelet production.[2,18] However, *Ptprj* KO mice have normal platelet counts, MKs from these mice display reduced spreading on collagen-, fibrinogen- and fibronectin-coated surfaces and are unable to migrate towards an SDF-1α gradient.[5] *Csk;Ptprj* double KO (DKO) mice also present normal mean platelet counts, demonstrating that the deletion of *Ptprj* rescues the platelet count phenotype of *Csk* KO mice, as well as MK counts in the bone marrow (BM).[2] Recently, biallelic loss-of-function mutations in *Ptprj* (g.48131608A>G and g.48158556delG) were described in patients, resulting in a novel form of inherited thrombocytopenia, characterized by impaired maturation of MKs and reduced platelet volume, further highlighting the importance of PTPRJ to MK development and function.[19]

We previously showed that phosphorylation of the C-terminal inhibitory tyrosine residues of SFKs was partially rescued in platelets lacking both Csk and PTPRJ, suggesting that another kinase can compensate for Csk.[2] We found that Csk homologous kinase (Chk, also known as megakaryocyte-associated tyrosine kinase, Matk), is upregulated in these platelets and thus might partially fulfil the function of Csk.[2] Chk shares approximately 50%

homology with Csk, with restricted expression in neuronal cells in the brain and hematopoietic cells. Chk was previously detected in platelets by Western blotting, but not by mass spectrometry-based approaches, suggesting low levels of expression.[20-22] This correlated with the lack of a platelet or hemostatic phenotype in *Chk* KO mice drawing into question the functional relevance of Chk in platelets.[23] Chk has been implicated in MK progenitor formation by using antisense oligonucleotides to reduce protein expression.[24] In addition, overexpression of Chk lead to a reduction in agonist-induced SFK activity in megakaryocytic cell lines,[25] and the protein was also implicated in cell spreading,[26] however, *in vivo* data is lacking.[23,27,28]

In this study, we have generated and analysed *Chk* KO mice alongside *Chk;Csk* DKO and *Chk;Csk;Ptprj* triple KO (TKO) mice, to determine if there is functional redundancy between Chk and Csk and whether the lack of PTPRJ can rescue MK and platelet phenotypes.

Methods

Mice

Matk^{tm1Sor} knockout (*Chk* KO) mice were from the Jackson Laboratories. *Csk*$^{fl/fl}$, *Ptprj*$^{fl/fl}$, and *Pf4-Cre*$^{+}$ mice were generated, as previously described.[29-31] All mice were on a C57BL/6 background. *Pf4-Cre*$^{+}$ mice were used as control mice. All procedures were undertaken with United Kingdom Home Office approval in accordance with the Animals (Scientific Procedures) Act of 1986.

Antibodies and reagents

Anti-CD42a antibody was from Abcam; anti-Shp1, anti-Shp1 p-Tyr564, anti-Shp2 and anti-Shp2 p-Tyr580 antibodies were from Cell Signaling Technology; anti-mouse TLT-1 Alexa Fluor-488 antibody was from R&D systems.[32] Fluorescein peanut agglutinin was from Vector Laboratories. Dasatinib was from LC laboratories, PP1 was from Calbiochem and PRT-060318 was from SynKinase. Other antibodies and reagents were previously described.[2]

Platelet preparation

Washed platelets were prepared as described.[2] Platelet concentration was normalized at 2 x 10^7/ml for spreading and flow cytometry analysis, and 5 x 10^8/ml for biochemical analysis.

Saline tail bleeding time assay

Mice were anesthetized using isoflurane and 3 mm of the tail tip was cut off. Immediately, tails were immersed in 0.9% isotonic saline at 37 °C. The time to complete arrest of bleeding (no blood flow for 1 minute) was determined. If on/off cycles of bleeding occurred, the sum of bleeding times within a 20-minute period was used. Otherwise, experiments were stopped after 20 minutes.

Immunohistochemistry, platelet functional assays and biochemistry

Immunohistochemistry, platelet adhesion, stimulation for flow cytometry and immunoblotting by ProteinSimple Wes are described in detail in the supplemental Methods.

Statistical analysis

Data presented are means ± standard deviation (SD). One-way or two-way ANOVA followed by appropriate *post-hoc* test were used to determine statistical significance ($P < .05$).

Results

Severe macrothrombocytopenia in *Chk;Csk* DKO mice

Constitutive *Chk* KO (CKO) mice were crossed with *Csk*$^{fl/fl}$*;Pf4-Cre*$^{+}$ mice, in which Csk was conditionally deleted, to generate *Chk;Csk* DKO mice. DKO mice were further crossed with *Ptprj*$^{fl/fl}$ mice to generate *Chk;Csk;Ptprj* TKO mice in which Chk is deleted in every cell, whereas Csk and PTPRJ are deleted in MKs, platelets and subsets of leukocytes due to leakiness of the *Pf4-Cre* transgene, as previously described.[18] We detected Chk expression in control mouse platelets by quantitative capillary electrophoresis-based immunoassays (ProteinSimple Wes), which was absent in CKO, DKO and TKO mice (Figure 1A-B). Csk expression was reduced to 6% in DKO and to 1% in TKO platelets compared to control platelets (Figure 1A-C). Surface expression of PTPRJ was reduced to 11% in TKO platelets, however, DKO platelets displayed a mean increase of 166% in PTPRJ surface expression, possibly as a compensatory feedback mechanism (Figure 1D). Platelet counts were normal in CKO mice, however DKO mice displayed severe thrombocytopenia with a 92% reduction in platelet counts compared to control mice (Figure 1E and Table S1). This is a further 27% decrease compared with *Csk* KO mice, previously reported to have a 65% reduction in platelet count.[2] Intriguingly, TKO mice had only a 34% reduction in platelet count compared with controls, demonstrating a partial rescue of the DKO phenotype in the absence of PTPRJ (Figure 1E). Mean platelet volume was not significantly different in CKO mice, whereas it was increased 49% in DKO mice and 23% in TKO mice (Figure 1F). The spleen/body weight ratio was also increased by 244% in DKO mice and 115% in TKO mice (Figure 1G), suggesting extramedullary hematopoiesis. These results demonstrate that while Csk can compensate for the loss of Chk in CKO mice, when both kinases are absent, DKO mice develop a more severe thrombocytopenia compared to *Csk* KO mice, suggesting redundancy in regulating platelet count.

Aberrant megakaryocyte counts and associated myelofibrosis in DKO and TKO mice

Histological analysis of main sites of thrombopoiesis, namely the bone marrow, spleen and lung, revealed major differences in MK counts in DKO and TKO mice. We found a 44% increase in MK count per field of view in TKO bone marrow and a 49% increase when counted the total number of MKs per section, but no difference in MK numbers in CKO or DKO bone marrow compared to control mice (Figure 2A, D-E). Notably, MKs in DKO and TKO bone marrow appeared atypical. Furthermore, we found an over 6-fold increase in MK numbers per field of view in the spleen of both DKO and TKO mice (Figure 2B and E). The total number of MKs per spleen section increased by over 13-fold in DKO and by over 8-fold in TKO mice (Figure 2D). A marginal increase in the number of $CD42b^+$ cells was observed in the lungs of DKO and TKO mice (Figure 2C-D), which may be MKs or MK fragments as a consequence of increased megakaryopoiesis and release from the bone marrow and spleens of these mice. We also observed associated paratrabecular and perivascular reticulin staining in the bone marrow and a marginal increase in reticulin staining in the spleen of DKO and TKO mice (Figure 2A-B), indicative of fibrosis.

Reduction in the level of GPVI and CLEC-2 in DKO and TKO platelets

To investigate whether changes in platelet count correlate with altered platelet receptors, we quantified surface levels of receptors responsible for platelet production and activation. We found a 21-24% increase in αIIbβ3 levels in DKO and TKO platelets, and 21% decrease in α2 levels in DKO platelets (Figure 3A). GPIbα levels were increased by 82% in DKO platelets, which plays a central role in regulating platelet size and count.[33] Surface expression of the ITAM-containing GPVI receptor was reduced by 77% and by 97% in DKO and TKO platelets, respectively (Figure 3A). Moreover, surface expression of the hemi-ITAM-containing CLEC-2 receptor was reduced by 43% and 79% in DKO and TKO platelets, respectively. Platelet

surface expression of the inhibitory ITIM-containing MPIG6B receptor was reduced by 23% in CKO platelets and increased by 44% in TKO platelets. These data suggest that Chk plays a role in regulating surface expression of ITAM-containing receptors, as previously established for Csk and PTPRJ.[2]

Increased platelet turnover and pre-activation in DKO and TKO mice

To further investigate the cause of thrombocytopenia in DKO and TKO mice, we assessed the fraction of immature reticulated, desialylated and pre-activated platelets in whole blood from these mice. All of these parameters were similar in CKO and control mice (Figure 3B-F). However, we found 4- and 2-fold increases in reticulated platelets in DKO and TKO mice respectively compared with control mice, suggesting a higher percentage of young platelets in the circulation of these mice (Figure 3B-C). Platelet staining with peanut agglutinin (PNA) lectin, which specifically binds to exposed galactose residues, was used as a marker of desialylation of surface glycans, and is associated with old platelets.[34] We found a 74% increase in PNA binding to DKO platelets, and a 50% increase to TKO platelets, compared to controls (Figure 3D-E). We next stained resting platelets for different activation markers. We observed a 52-fold increase in the percentage of P-selectin positive platelets in TKO blood (Figure 3F), suggesting platelet pre-activation. Notably, we detected 8- and 7-fold increases in surface TLT-1 levels in DKO and TKO platelets, respectively compared to control (Figure 3F), providing further evidence of platelet pre-activation in these mice. We also observed 2- and 5-fold increases in fibrinogen binding in DKO and TKO platelets, respectively, compared with platelets from control mice, suggesting the integrin αIIbβ3 was in a high affinity, active conformation in a proportion of these platelets. We found only a minor increase in the percentage of Annexin V positive platelets in blood from DKO mice (Figure 3F). Increased

megakaryocyte counts and immature platelet fraction suggests impaired platelet production in DKO mice, which was partially restored in TKO mice.

Platelet functional defects in DKO mice are rescued in TKO mice

Due to the severe thrombocytopenia in DKO mice, we were only able to test platelet function in a limited set of assays. Platelet α-granule secretion and integrin αIIbβ3 activation were assessed by measuring P-selectin and TLT-1 surface expression and fibrinogen binding, respectively by flow cytometry. PAR4 peptide-stimulated CKO platelets expressed similar increase in P-selectin and TLT-1 levels and displayed comparable elevation of fibrinogen binding as stimulated control platelets (Figure 4A and Figure S1). In contrast, DKO platelets exhibited significant impairment in staining for all three markers (Figure 4A). Interestingly, PAR4 peptide-stimulated TKO platelets showed a similar increase in P-selectin expression and fibrinogen binding as control platelet, despite higher basal expressions of these markers in whole blood (Figure 3F), however there was a minor reduction in TLT-1 expression (Figure 4A), presumably as a consequence of activation of inhibitory mechanisms.[32]

We next analysed platelet spreading on a fibrinogen coated surface, as a means of assessing integrin αIIbβ3 function. Resting platelets were either directly plated on fibrinogen, or were pre-activated with 0.1 U/ml thrombin prior to plating. CKO platelets spread comparably to control platelets, whereas DKO platelets displayed a 28% increase in spreading (Figure 4B-C). However, in the presence of thrombin, there was no significant difference between control and DKO platelets. Although TKO platelets spread to a similar extent as control platelets, the morphology of thrombin activated TKO platelets was different compared to control platelets, with reduced lamellipodia and stress fibre formation (Figure 4B).

We next assessed the haemostasis in the various mouse models using the saline tail bleeding assay. We found no significant difference in bleeding time of CKO mice compared

with control mice (Figure 4D). In agreement with the 92% reduction in platelet count in DKO mice (Figure 1E), we observed significant bleeding in these mice (Figure 4D). This bleeding phenotype was rescued in TKO mice, which displayed no significant difference in bleeding time compared with control mice (Figure 4D). We conclude that the partially rescued platelet count in combination with the almost normal platelet reactivity in response to thrombin receptor stimulation is sufficient to restore haemostatic function in TKO mice.

Partial rescue of Src and Fyn inhibitory tyrosine phosphorylation in TKO platelets

To study the biochemical consequences of ablating Chk, Csk and PTPRJ, we assessed tyrosine phosphorylation of SFKs in resting platelets by a capillary electrophoresis-based immunoassay. We measured phosphorylation of the activation loop tyrosine residue of SFKs (Src p-Tyr418), an indirect indicator of SFK activity, which was normal in CKO and DKO, and increased 75% in TKO platelets (Figure 5A-B), possibly due to increased PTPRJ expression, which can dephosphorylate Src p-Tyr418 and attenuate activity (Figure 1D). We then measured phosphorylation of the C-terminal inhibitory tyrosine residues of Src, Lyn and Fyn, which binds intra-molecularly with their SH2 domain, locking the kinases in an inactive conformation. We observed an 80-92% decrease of Src p-Tyr529, Lyn p-Tyr507 and Fyn p-Tyr530 in DKO platelets compared with controls (Figure 5A-B). There was a 4-fold increase in Src p-Tyr529 and a 2-fold increase in Fyn p-Tyr530 in TKO platelets compared to DKO platelets, but no significant difference in Lyn p-Tyr507. These residues were phosphorylated to the same extent in CKO platelets. These findings suggest that another kinase can phosphorylate these inhibitory tyrosine residues in the absence of Chk and Csk. In addition, we found that Src, Lyn and Fyn all exhibited some degree of regulation on the protein level in DKO or TKO platelets. Whereas Src levels were increased by 134% in DKO platelets, Lyn and Fyn levels were reduced by 65% and 34%, respectively in TKO platelets compared to

controls (Figure 5A-B). Moreover, expression of the tyrosine kinase Syk was also found to be reduced in TKO platelets by 37%.

We next assessed the regulation of the cytosolic tyrosine phosphatases Shp1 and Shp2, both of which contain two conserved C-terminal tyrosine residues, phosphorylation of which has been implicated in regulating downstream signalling.[35-37] We found Shp1 p-Tyr564 to be increased by 6- and 10-fold in DKO and TKO platelets, respectively. However, DKO platelets also showed a 3-fold increase in Shp1 protein levels. Shp2 p-Tyr580 was increased by 5-fold in DKO platelets and 7-fold in TKO platelets (Figure 5A-B). These findings demonstrate that SFKs lie upstream of Shp1 and Shp2, acting either directly or indirectly, to activate these phosphatases.

SFKs auto-phosphorylate their C-terminal inhibitory tyrosine residues

To explore which other kinases phosphorylate the C-terminal tyrosine residues of SFKs, we incubated control and TKO platelets with two different SFK inhibitors, namely dasatinib and PP1, and the Syk kinase inhibitor PRT-060318.[16,38] Dasatinib and PP1 significantly reduced Src p-Tyr418 in control and TKO platelets, whereas PRT-060318 had only a minor effect, as expected. We found that dasatinib reduced Src p-Tyr529, Lyn p-Tyr507 and Fyn p-Tyr530 in TKO platelets by 52-62%, and PP1 reduced phosphorylation of these sites by 64-73% (Figure 6A-B). These findings suggest that SFKs themselves are able to phosphorylate their C-terminal inhibitory tyrosine residues in the absence of Chk and Csk, thus auto-inhibiting their activity (Figure 7). However, PRT-060318 had no significant effect on phosphorylation of these residues in TKO platelets, suggesting Syk plays no role in phosphorylating these residues.

Discussion

In the present study, we investigated the physiological functions of Chk, Csk and PTPRJ in platelets. By analysing mice lacking Chk alone, or in combination with Csk and PTPRJ, we demonstrate that Chk and Csk have redundant functions inhibiting SFKs in the MK lineage (Figure 7), with Csk playing the dominant role, and that PTPRJ plays a central role in both activating and attenuating SFK activity. DKO mice developed severe macrothrombocytopenia with a 92% drop in platelet count, elevated MK numbers and immature platelet fraction, pointing to disruption of platelet production. Platelet counts in DKO mice were considerably lower than in *Csk* KO mice, whereas MK numbers in the spleen and immature platelet fraction were double (Table 1).[2] These phenotypes suggest that Csk can fully compensate for the absence of Chk in MKs and platelets, whereas Chk can compensate only in part in the absence of Csk. DKO mice revealed that Chk and Csk are essential for platelet production. TKO mice showed partially restored platelet counts, elevated MK numbers in the bone marrow and spleen, and an immature platelet fraction that was between control and DKO mice. These findings together with our previous report demonstrating rescued platelet counts in the *Csk;Ptprj* DKO mice compared to *Csk* KO mice, highlight that by controlling the extent of phosphorylation of the C-terminal inhibitory tyrosine residues of SFKs, PTPRJ plays a central role in regulating platelet counts and activation (Figure 7, Table 1).[2]

Biallelic loss-of-function mutations in *Ptprj* has recently been suggested to cause a novel form of inherited thrombocytopenia humans.[19] Although most of the human findings correlate with results from *Ptprj*-deficient mice, significant reduction in the platelet count is not observed in constitutive *Ptprj* loss-of-function transmembrane KO mice or in conditional KO mice generated with either the *Pf4-Cre* or *Gp1ba-Cre* transgenes (Figure S2).[2,5,18] Although the cause of these apparent differences is not known, we hypothesize this is primarily due to epigenetic effects and modifier loci in the patients that is not the case in inbred C57Bl/6

mice. Of note, ablation of *Ptprj* in zebrafish resulted in only a minor drop in thrombocyte counts.[19]

One of the consequences of increased MK count is the development of myelofibrosis, which was observed in the bone marrow of DKO and TKO mice, but not in *Csk* KO or *Csk,Ptprj* DKO mice (Table 1). Primary myelofibrosis is a rare heterogeneous disorder with poor prognosis in which somatic mutations drive clonal expansion of hematopoietic stem cells; and is characterized by bone marrow fibrosis, MK proliferation and atypia, extramedullary hematopoiesis and splenomegaly. Since MKs play a central role in the development of myelofibrosis,[39,40] and PTPRJ plays a central role in regulating MK function,[2,5,19] our findings highlight PTPRJ as a potential novel target either alone or in combination with existing therapies in the treatment of myeloproliferative neoplasms and myelofibrosis.

Phosphorylation of C-terminal inhibitory tyrosine residues was barely detectable in DKO platelets, which increased significantly in Src and Fyn in TKO platelets, demonstrating phosphorylation in the absence of the only two known kinases which are able to phosphorylate these sites.[41] It also illustrates that PTPRJ must constitutively dephosphorylate these residues, even in resting platelets, maintaining a pool of active SFKs in platelets, facilitating rapid activation following vascular injury. We observed that the levels of total Lyn were reduced by 65% in TKO platelets, which may explain the lack of increase in phosphorylation of Tyr507 in its C-terminal tail. The mechanism for the reduction of Lyn expression is not known, but likely involves degradation by the E3 ubiquitin ligase c-Cbl, as previously described in immune cells.[42] Inhibition of an analog-sensitive variant of Csk induced robust c-Cbl phosphorylation and rapid LynA degradation in macrophages.[42] In spite of the lack of C-terminal inhibitory phosphorylation of SFKs in DKO platelets, we did not observe a significant increase in their activation loop phosphorylation. The reason for this could be the significant increase in PTPRJ levels in these platelets, which is able to dephosphorylate the activation loop tyrosine of SFKs,

in addition to the C-terminal inhibitory tyrosine residues.[2,6] The increase in Shp1 p-Tyr564 and Shp2 p-Tyr580 suggests elevated inhibitory signaling in DKO and TKO platelets. Shp1 phosphorylation has previously been shown to be increased in macrophages expressing a hyperactive variant of Lyn and to be diminished in *Lyn* KO cells.[43] Specifically, Lyn has been demonstrated to be the predominant kinase phosphorylating Shp1 p-Tyr564 site.[44] Src was also shown to directly phosphorylate Shp1.[35] In addition, thrombin induced Shp1 phosphorylation was absent in the presence of SFK inhibitors in platelets.[45] Similarly, Shp2 p-Tyr580 may also be a direct substrate of SFKs. These studies suggest that SFK activity was indeed elevated in DKO platelets, despite normal phosphorylation of the SFK activation loop tyrosine residue.

Inhibitor studies using TKO platelets indicate that SFKs are capable of auto-phosphorylating their C-terminal tails and presumably auto-inhibiting activity (Figure 7B). In addition to SFKs, both PP1 and Dasatinib inhibit Csk at higher concentrations, whereas the latter also blocks the activity of the tyrosine kinases Btk, Tec and Abl.[46-48] Although, we cannot exclude the possibility that inhibition of Btk, Tec or Abl may contribute to the reduction of C-terminal inhibitory site phosphorylation of SFKs in the Dasatinib-treated samples, the activity of these kinases should not be affected in the PP1-treated samples. Interestingly, we also observed a significant decrease in the inhibitory site phosphorylation of Src, Lyn and Fyn in control platelets incubated with SFK inhibitors, which may be the consequence of the combined decrease in SFK and Csk activities. We hypothesize that the auto-inhibitory function is particularly important as a means of preventing excessive and prolonged SFK activation in both unstimulated and ligand-mediated receptor clustering conditions.

As SFKs are ubiquitously expressed, auto-phosphorylation of their C-terminal inhibitory site has previously not appreciated, broad implications for several cell types.[41,49] Indeed, deletion of Chk alone had no detectable effect on phosphorylation of the C-terminal

inhibitory tyrosine residues of SFKs in platelets, demonstrating that Csk and auto-inhibition is sufficient to prevent aberrant SFK activation. Residual SFK-mediated auto-phosphorylation of the inhibitory tyrosine residues in the absence of Chk, Csk and PTPRJ correlated with normal bleeding in these mice, providing evidence of the physiological relevance of this mechanism. The kinetics of phosphorylation of these two regulatory tyrosine residues requires further investigation to better understand how SFKs auto-regulate their activity. Previous work from T cells has revealed a complex interplay between membrane localization and phosphorylation of these residues in T cell receptor signalling, requiring further investigation in platelets.[50]

Both DKO and TKO platelets showed signs of pre-activation in the absence of stimuli, highlighted by increased TLT-1 expression and fibrinogen binding. Interestingly, in response to PAR4 stimulation, TKO platelets were able to secrete their granules and bind fibrinogen similarly to control platelets, possibly due to the remaining inhibitory phosphorylation of SFKs. This may also be the result of elevated Shp1 and Shp2 inhibitory activity, via the ITIM-containing receptor MPIG6B.[2,51-53] In contrast, DKO platelets lacking phosphorylation of the C-terminal inhibitory tyrosine residues of SFKs were unable to respond to thrombin receptor stimulation. As a consequence of reduced platelet count and reactivity, DKO mice exhibited significantly increased tail bleeding, whereas TKO mice responded similar to control mice in this assay. Increased PNA staining of platelets from DKO and TKO mice, indicative of increased de-sialylation of surface glycans, suggested aberrant platelet turnover, with a population of platelets remaining in the circulation longer than normal. Intriguingly, we observed significant downregulation of (hemi-)ITAM containing receptors in TKO platelets with only 3% of GPVI levels and 21% of CLEC-2 levels. These findings reinforce the key role of SFKs in regulating surface GPVI and CLEC-2 levels previously observed in *Csk* KO and *Csk;Ptprj* DKO platelets (Table 1),[2] which might be explained by potentially increased

activation of c-Cbl.[42] Alternatively, decreased GPVI and CLEC-2 levels might be a consequence of platelet pre-activation. Of note, concomitant deletion of these (hemi-)ITAM-containing receptors in mice has previously been shown to result in a profound bleeding diathesis,[54] which is likely counter-acted by elevated SFK activity in TKO platelets.

In summary, we demonstrated a critical role for Chk, Csk and PTPRJ in platelet homeostasis. Although, Chk was previously implicated in MK maturation, *in vivo* evidence was lacking.[23-28] In our study, we demonstrate no megakaryocyte or platelet functional defects in CKO mice. However, DKO mice developed severe macrothrombocytopenia, elevated MK counts and immature platelet fraction and myelofibrosis, pointing to an important role of Chk and Csk in regulation of platelet counts. Importantly, additional deletion of PTPRJ from MKs and platelets partially corrected platelet counts and immature platelet fraction. As tyrosine phosphatases are increasingly considered druggable, targeting PTPRJ might serve as an alternative strategy to regulate platelet counts in instances of high SFK activity.[55] We have also identified a novel inhibitory mechanism, involving auto-phosphorylation of the C-terminal inhibitory tyrosine residues of SFKs, which likely plays an important role in regulating these kinases in other cell types, including immune and cancer cells. In platelets, the partially rescued inhibitory phosphorylation and elevated platelet counts preserved the ability of platelets to respond to stimuli and restored haemostasis.

Acknowledgments

The authors acknowledge Arthur Weiss (University of California, San Francisco, California, USA) for providing *Ptprj*$^{fl/fl}$ mice,[30] Alexander Tarakhovsky (The Rockefeller University, New York, USA) for providing *Csk*$^{fl/fl}$ mice,[29] Jeremy Pike (University of Birmingham, Birmingham, UK) for providing the KINME analysis software, Gordon Stamp, Mahrokh Nohadani and Rieda Ahmad (Advance Histopathology Laboratory Ltd, London, UK) for performing histology analysis and all members of the Birmingham Biomedical Sciences Unit for maintenance of mouse colonies. The authors thank Oreste Acuto (University of Oxford, Oxford, UK) for intellectual contributions.

Z.N. and J.M. are British Heart Foundation (BHF) postdoctoral research associates (RG/15/13/31673) and A.M. is a BHF Intermediate Basic Science Research Fellow (FS/15/58/31784). This work was supported by BHF Senior Basic Science Research Fellowship FS/13/1/29894 and BHF Programme Grant RG/15/13/31673 (Y.A.S.) and by a Research Development Fund provided by the University of Birmingham (Z.N.).

Authorship Contributions

Contribution: Y.A.S. provided conceptualization; Z.N., J.M. and Y.A.S. provided methodology; Z.N., J.M., V.-S.I. and Y.A.S. provided the investigation; Y.A.S. provided resources; A.M. and Y.A.S. provided mouse models and reagents; Z.N. and Y.A.S. wrote the original draft; Z.N., J.M., V.-S.I., A.M. and Y.A.S. performed review and editing; Y.A.S. provided supervision; Z.N. and Y.A.S. provided funding acquisition.

Conflict of Interest Disclosures

The authors declare no competing financial interests.

References

1. Senis YA, Mazharian A, Mori J. Src family kinases: at the forefront of platelet activation. *Blood*. 2014;124(13):2013-2024.
2. Mori J, Nagy Z, Di Nunzio G, et al. Maintenance of murine platelet homeostasis by the kinase Csk and phosphatase CD148. *Blood*. 2018;131(10):1122-1144.
3. Ming Z, Hu Y, Xiang J, Polewski P, Newman PJ, Newman DK. Lyn and PECAM-1 function as interdependent inhibitors of platelet aggregation. *Blood*. 2011;117(14):3903-3906.
4. Mori J, Wang YJ, Ellison S, et al. Dominant role of the protein-tyrosine phosphatase CD148 in regulating platelet activation relative to protein-tyrosine phosphatase-1B. *Arterioscler Thromb Vasc Biol*. 2012;32(12):2956-2965.
5. Senis YA, Tomlinson MG, Ellison S, et al. The tyrosine phosphatase CD148 is an essential positive regulator of platelet activation and thrombosis. *Blood*. 2009;113(20):4942-4954.
6. Ellison S, Mori J, Barr AJ, Senis YA. CD148 enhances platelet responsiveness to collagen by maintaining a pool of active Src family kinases. *J Thromb Haemost*. 2010;8(7):1575-1583.
7. Stepanek O, Kalina T, Draber P, et al. Regulation of Src family kinases involved in T cell receptor signaling by protein-tyrosine phosphatase CD148. *J Biol Chem*. 2011;286(25):22101-22112.
8. Pera IL, Iuliano R, Florio T, et al. The rat tyrosine phosphatase eta increases cell adhesion by activating c-Src through dephosphorylation of its inhibitory phosphotyrosine residue. *Oncogene*. 2005;24(19):3187-3195.
9. Turro E, Greene D, Wijgaerts A, et al. A dominant gain-of-function mutation in universal tyrosine kinase SRC causes thrombocytopenia, myelofibrosis, bleeding, and bone pathologies. *Sci Transl Med*. 2016;8(328):328ra330.
10. De Kock L, Thys C, Downes K, et al. De novo variant in tyrosine kinase SRC causes thrombocytopenia: case report of a second family. *Platelets*. 2019:1-4.
11. Lannutti BJ, Drachman JG. Lyn tyrosine kinase regulates thrombopoietin-induced proliferation of hematopoietic cell lines and primary megakaryocytic progenitors. *Blood*. 2004;103(10):3736-3743.
12. Lannutti BJ, Minear J, Blake N, Drachman JG. Increased megakaryocytopoiesis in Lyn-deficient mice. *Oncogene*. 2006;25(23):3316-3324.
13. Murphy AJ, Bijl N, Yvan-Charvet L, et al. Cholesterol efflux in megakaryocyte progenitors suppresses platelet production and thrombocytosis. *Nat Med*. 2013;19(5):586-594.
14. Severin S, Nash CA, Mori J, et al. Distinct and overlapping functional roles of Src family kinases in mouse platelets. *J Thromb Haemost*. 2012;10(8):1631-1645.
15. Lannutti BJ, Blake N, Gandhi MJ, Reems JA, Drachman JG. Induction of polyploidization in leukemic cell lines and primary bone marrow by Src kinase inhibitor SU6656. *Blood*. 2005;105(10):3875-3878.
16. Mazharian A, Ghevaert C, Zhang L, Massberg S, Watson SP. Dasatinib enhances megakaryocyte differentiation but inhibits platelet formation. *Blood*. 2011;117(19):5198-5206.
17. Jarocha D, Vo KK, Lyde RB, Hayes V, Camire RM, Poncz M. Enhancing functional platelet release in vivo from in vitro-grown megakaryocytes using small molecule inhibitors. *Blood Adv*. 2018;2(6):597-606.
18. Nagy Z, Vogtle T, Geer MJ, et al. The Gp1ba-Cre transgenic mouse: a new model to delineate platelet and leukocyte functions. *Blood*. 2018.

19. Marconi C, Di Buduo CA, LeVine K, et al. A new form of inherited thrombocytopenia caused by loss-of-function mutations in PTPRJ. *Blood*. 2018.
20. Hirao A, Hamaguchi I, Suda T, Yamaguchi N. Translocation of the Csk homologous kinase (Chk/Hyl) controls activity of CD36-anchored Lyn tyrosine kinase in thrombin-stimulated platelets. *EMBO J*. 1997;16(9):2342-2351.
21. Burkhart JM, Vaudel M, Gambaryan S, et al. The first comprehensive and quantitative analysis of human platelet protein composition allows the comparative analysis of structural and functional pathways. *Blood*. 2012;120(15):e73-82.
22. Zeiler M, Moser M, Mann M. Copy number analysis of the murine platelet proteome spanning the complete abundance range. *Mol Cell Proteomics*. 2014;13(12):3435-3445.
23. Hamaguchi I, Yamaguchi N, Suda J, et al. Analysis of CSK homologous kinase (CHK/HYL) in hematopoiesis by utilizing gene knockout mice. *Biochem Biophys Res Commun*. 1996;224(1):172-179.
24. Avraham S, Jiang S, Ota S, et al. Structural and functional studies of the intracellular tyrosine kinase MATK gene and its translated product. *J Biol Chem*. 1995;270(4):1833-1842.
25. Price DJ, Rivnay B, Avraham H. CHK down-regulates SCF/KL-activated Lyn kinase activity in Mo7e megakaryocytic cells. *Biochem Biophys Res Commun*. 1999;259(3):611-616.
26. Hirao A, Huang XL, Suda T, Yamaguchi N. Overexpression of C-terminal Src kinase homologous kinase suppresses activation of Lyn tyrosine kinase required for VLA5-mediated Dami cell spreading. *J Biol Chem*. 1998;273(16):10004-10010.
27. Samokhvalov I, Hendrikx J, Visser J, Belyavsky A, Sotiropolous D, Gu H. Mice lacking a functional chk gene have no apparent defects in the hematopoietic system. *Biochem Mol Biol Int*. 1997;43(1):115-122.
28. Lee BC, Avraham S, Imamoto A, Avraham HK. Identification of the nonreceptor tyrosine kinase MATK/CHK as an essential regulator of immune cells using Matk/CHK-deficient mice. *Blood*. 2006;108(3):904-907.
29. Schmedt C, Saijo K, Niidome T, Kuhn R, Aizawa S, Tarakhovsky A. Csk controls antigen receptor-mediated development and selection of T-lineage cells. *Nature*. 1998;394(6696):901-904.
30. Katsumoto TR, Kudo M, Chen C, et al. The phosphatase CD148 promotes airway hyperresponsiveness through SRC family kinases. *J Clin Invest*. 2013;123(5):2037-2048.
31. Tiedt R, Schomber T, Hao-Shen H, Skoda RC. Pf4-Cre transgenic mice allow the generation of lineage-restricted gene knockouts for studying megakaryocyte and platelet function in vivo. *Blood*. 2007;109(4):1503-1506.
32. Smith CW, Raslan Z, Parfitt L, et al. TREM-like transcript 1: a more sensitive marker of platelet activation than P-selectin in humans and mice. *Blood Adv*. 2018;2(16):2072-2078.
33. Kanaji T, Ware J, Okamura T, Newman PJ. GPIbalpha regulates platelet size by controlling the subcellular localization of filamin. *Blood*. 2012;119(12):2906-2913.
34. Li J, van der Wal DE, Zhu G, et al. Desialylation is a mechanism of Fc-independent platelet clearance and a therapeutic target in immune thrombocytopenia. *Nat Commun*. 2015;6:7737.
35. Frank C, Burkhardt C, Imhof D, et al. Effective dephosphorylation of Src substrates by SHP-1. *J Biol Chem*. 2004;279(12):11375-11383.
36. Lu W, Gong D, Bar-Sagi D, Cole PA. Site-specific incorporation of a phosphotyrosine mimetic reveals a role for tyrosine phosphorylation of SHP-2 in cell signaling. *Mol Cell*. 2001;8(4):759-769.
37. Zhang ZS, Shen K, Lu W, Cole PA. Regulation of SHP-1 activity by phosphorylation of the C-terminal tail tyrosine residues, Y536 and Y564. *Biophysical Journal*. 2003;84(2):28a-28a.

38. Reilly MP, Sinha U, Andre P, et al. PRT-060318, a novel Syk inhibitor, prevents heparin-induced thrombocytopenia and thrombosis in a transgenic mouse model. *Blood*. 2011;117(7):2241-2246.
39. Malara A, Abbonante V, Zingariello M, Migliaccio A, Balduini A. Megakaryocyte Contribution to Bone Marrow Fibrosis: many Arrows in the Quiver. *Mediterr J Hematol Infect Dis*. 2018;10(1):e2018068.
40. Kramann R, Schneider RK. The identification of fibrosis-driving myofibroblast precursors reveals new therapeutic avenues in myelofibrosis. *Blood*. 2018;131(19):2111-2119.
41. Roskoski R, Jr. Src protein-tyrosine kinase structure, mechanism, and small molecule inhibitors. *Pharmacol Res*. 2015;94:9-25.
42. Freedman TS, Tan YX, Skrzypczynska KM, et al. LynA regulates an inflammation-sensitive signaling checkpoint in macrophages. *Elife*. 2015;4.
43. Harder KW, Parsons LM, Armes J, et al. Gain- and loss-of-function Lyn mutant mice define a critical inhibitory role for Lyn in the myeloid lineage. *Immunity*. 2001;15(4):603-615.
44. Xiao W, Ando T, Wang HY, Kawakami Y, Kawakami T. Lyn- and PLC-beta3-dependent regulation of SHP-1 phosphorylation controls Stat5 activity and myelomonocytic leukemia-like disease. *Blood*. 2010;116(26):6003-6013.
45. Ma P, Cierniewska A, Signarvic R, et al. A newly identified complex of spinophilin and the tyrosine phosphatase, SHP-1, modulates platelet activation by regulating G protein-dependent signaling. *Blood*. 2012;119(8):1935-1945.
46. Hantschel O, Rix U, Schmidt U, et al. The Btk tyrosine kinase is a major target of the Bcr-Abl inhibitor dasatinib. *Proc Natl Acad Sci U S A*. 2007;104(33):13283-13288.
47. Rix U, Hantschel O, Durnberger G, et al. Chemical proteomic profiles of the BCR-ABL inhibitors imatinib, nilotinib, and dasatinib reveal novel kinase and nonkinase targets. *Blood*. 2007;110(12):4055-4063.
48. Bain J, Plater L, Elliott M, et al. The selectivity of protein kinase inhibitors: a further update. *Biochem J*. 2007;408(3):297-315.
49. Martin GS. The hunting of the Src. *Nat Rev Mol Cell Biol*. 2001;2(6):467-475.
50. Nika K, Soldani C, Salek M, et al. Constitutively active Lck kinase in T cells drives antigen receptor signal transduction. *Immunity*. 2010;32(6):766-777.
51. Mazharian A, Wang YJ, Mori J, et al. Mice lacking the ITIM-containing receptor G6b-B exhibit macrothrombocytopenia and aberrant platelet function. *Sci Signal*. 2012;5(248):ra78.
52. Geer MJ, van Geffen JP, Gopalasingam P, et al. Uncoupling ITIM receptor G6b-B from tyrosine phosphatases Shp1 and Shp2 disrupts murine platelet homeostasis. *Blood*. 2018;132(13):1413-1425.
53. Hofmann I, Geer MJ, Vogtle T, et al. Congenital macrothrombocytopenia with focal myelofibrosis due to mutations in human G6b-B is rescued in humanized mice. *Blood*. 2018;132(13):1399-1412.
54. Bender M, May F, Lorenz V, et al. Combined in vivo depletion of glycoprotein VI and C-type lectin-like receptor 2 severely compromises hemostasis and abrogates arterial thrombosis in mice. *Arterioscler Thromb Vasc Biol*. 2013;33(5):926-934.
55. Senis YA, Barr AJ. Targeting Receptor-Type Protein Tyrosine Phosphatases with Biotherapeutics: Is Outside-in Better than Inside-Out? *Molecules*. 2018;23(3).

Table 1. Summary of *Chk, Csk and Ptprj* knockout mouse phenotypes

Phenotype	*Genotype*					
	Chk KO	***Csk KO*[2]**	***Ptprj KO*[2,5]**	***Chk; Csk DKO***	***Csk; Ptprj DKO*[2]**	***Chk; Csk; Ptprj TKO***
Platelet count	—	↓↓	—	↓↓↓	—	↓
Reticulated platelets	—	↑	—	↑↑↑	↑	↑
MK count						
Bone marrow	—	↑	—	—	—	↑
Spleen	—	↑↑	↑	↑↑↑	↑↑	↑↑↑
Splenomegaly	—	↑	—	↑↑↑	↑	↑
Myelofibrosis in bone marrow	—	—	—	↑↑	—	↑↑
SFK activity	—	↑	↓↓	—	↑↑	↑
Platelet receptor expression						
GPIbα	—	↑↑	—	↑↑	↑	—
GPVI	—	↓↓	↓	↓↓	↓↓	↓↓↓
CLEC-2	—	↓	—	↓	↓↓	↓↓
MPIG6b-B	↓	↑↑	—	—	↑↑	↑↑
Platelet spreading (fibrinogen)	—	↑	↓	↑	—	—
Bleeding	—	↑	—	↑↑↑	↑↑	—

↑ upregulated, ↓ downregulated, — normal

Figures

Figure 1. Severe macrothrombocytopenia in DKO mice is partially rescued in TKO mice. (A) Representative blots of capillary-based immunoassays on platelet lysates with the indicated antibodies. (B) Representative data from (A) displayed as electropherograms. (C) Quantification of peak areas of Csk signal from (A-B), n = 6 mice/genotype. (D) Median fluorescence intensity (MFI) measured in αIIb^+ cells co-stained for PTPRJ in blood, n = 6 mice/genotype. (E) Platelet counts, n = 14 mice/genotype. (F) Platelet volumes, n = 14 mice/genotype. (G) Spleen/body weight ratio, n = 15 mice/genotype. *Chk*$^{-/-}$ (CKO), *Chk*$^{-/-}$*;Csk*$^{fl/fl}$*;Pf4-Cre*$^+$ (DKO), *Chk*$^{-/-}$*;Csk*$^{fl/fl}$*;Ptprj*$^{fl/fl}$*;Pf4-Cre*$^+$ (TKO).

Asterisks refer to significant difference compared to control, or significant difference between DKO and TKO. $^{**}P < 0.01$, $^{***}P < 0.001$, one-way ANOVA with Sidak's test; mean ± SD.

Figure 2. Aberrant megakaryocyte counts and myelofibrosis in DKO and TKO mice. (A-C) Histological sections of mouse (A) bone marrow, (B) spleen and (C) lung of the indicated genotypes stained with H&E, the megakaryocytic marker CD42b or reticulin. MKs are highlighted by yellow arrows. (D) Total number of MKs per section in the bone marrow and spleen, and total number of $CD42b^+$ cell fragments per section in the lung, n = 5 mice/genotype. (E) MK numbers per field of view in the indicated organs, n = 5 mice/genotype (mean of 15 fields/mouse). Analysis of MK numbers was performed in a double-blinded manner.

$^{*}P < 0.05$, $^{**}P < 0.01$, $^{***}P < 0.001$, one-way ANOVA with Sidak's test; mean ± SD.

Figure 3. Reduced expression of (hemi-)ITAM-containing receptors, elevated immature platelet fraction and platelet activation markers in DKO and TKO mice. (A) Median fluorescence intensity (MFI) measured in $\alpha IIb\beta3^+$ cells or αIIb^+ cells co-stained for the

indicated proteins in blood, n = 6 mice/genotype. (B) Representative image of reticulated platelet population as measured by flow cytometry. αIIb^+ platelets in whole blood were gated and the percentage of reticulated platelets was determined in gate P1 (in red), in dot plot diagram forward scatter (FSC) vs RNA dye (Thiazole Orange). (C) Percentage of reticulated platelets as determined in (B). (D) Representative image of desialylated platelet population. αIIb^+ platelets in whole blood were gated and the percentage of desialylated platelets was determined in gate P1 (in red), in dot plot diagram forward scatter (FSC) vs peanut agglutinin (PNA) lectin. (E) Percentage of desialylated platelets as determined in (D). (F) Percentage of P-selectin$^+\alpha IIb^+$, TLT-1$^+\alpha IIb^+$, fibrinogen$^+\alpha IIb^+$, or Annexin V$^+\alpha IIb^+$ cells in blood as determined by flow cytometry, n = 6 mice/genotype.

*$P < 0.05$, **$P < 0.01$, ***$P < 0.001$, one-way ANOVA with Sidak's test; mean ± SD.

Figure 4. Defective platelet activation and hemostasis in DKO mice is restored in TKO mice. (A) Anti-P-selectin-FITC, anti-TREM (triggering receptor expressed on myeloid cells)-like transcript 1 (TLT-1)-FITC and fibrinogen-488 binding to washed platelets (2 x 10^7/ml) following stimulation with or without PAR4 peptide (AYPGKF) (100 μM or 500 μM, 20 min, room temperature) was measured by flow cytometry. The fold increase of the median fluorescence intensity (MFI) relative to the corresponding unstimulated platelets was calculated, n = 5-7 mice/genotype. (B) Representative phalloidin-stained images of resting (basal) and thrombin-stimulated (0.1 Unit/ml, 5 minutes) platelets spread on fibrinogen-coated cover-slips (100 μg/ml, 45 minutes, 37°C, scale bar: 5 μm). (C) Mean surface area of individual platelets quantified by KNIME software, n = 6 mice/genotype (200 to 450 platelets/condition). (D) Hemostatic response was measured in saline tail bleeding assay by an excision of a 3-mm portion of the tail tip followed by immersion of the tail in 0.9% isotonic

saline at 37 °C. Plotted is the time to complete arrest of bleeding. Experiments were conducted in a double-blinded manner, n = 16 mice/genotype.

*P < 0.05, **P < 0.01, ***P < 0.001, one-way ANOVA with Sidak's test; mean ± SD.

Figure 5. Partial rescue of Src and Fyn inhibitory tyrosine phosphorylation in TKO platelets. (A) Representative blots of capillary-based immunoassays on lysates of resting platelets with the indicated antibodies. (B) Quantification of peak areas, n = 6 mice/genotype.

*P < 0.05, **P < 0.01, ***P < 0.001, one-way ANOVA with Sidak's test; mean ± SD.

Figure 6. SFKs auto-phosphorylate their C-terminal inhibitory tyrosine residues.

(A) Representative blots of capillary-based immunoassays on platelet lysates with the indicated antibodies. Lysates were generated from platelets incubated with DMSO, 50 nM dasatinib, 10 μM PP1, or 3 μM PRT-060318 for 15 min, room temperature. (B) Quantification of peak areas, n = 6 mice/genotype.

Asterisks refer to significant difference compared to DMSO-treated control samples within genotypes. *P < 0.05, **P < 0.01, ***P < 0.001, two-way ANOVA with Sidak's test; mean ± SD.

Figure 7. Revised model of regulation of SFKs in the megakaryocyte lineage.

(A) Src family kinase (SFK) activity is tightly regulated by the coordinated action of the tyrosine kinases Csk and Chk, the receptor-type tyrosine phosphatase PTPRJ, and SFKs themselves. Csk and Chk negatively regulate SFK activity, whereas PTPRJ and SFKs are dual positive and negative regulators of SFKs. (B) SFKs auto-regulate their catalytic activity through the trans-phosphorylation of conserved tyrosine residues in the activation loop and C-terminal tail. (C) An equilibrium of different states of SFKs is established in resting and

activated platelets through the interplay of these tyrosine kinases and phosphatase, as indicated. This is dependent on the concentrations, proximity and catalytic activities of these enzymes.

Figure 1

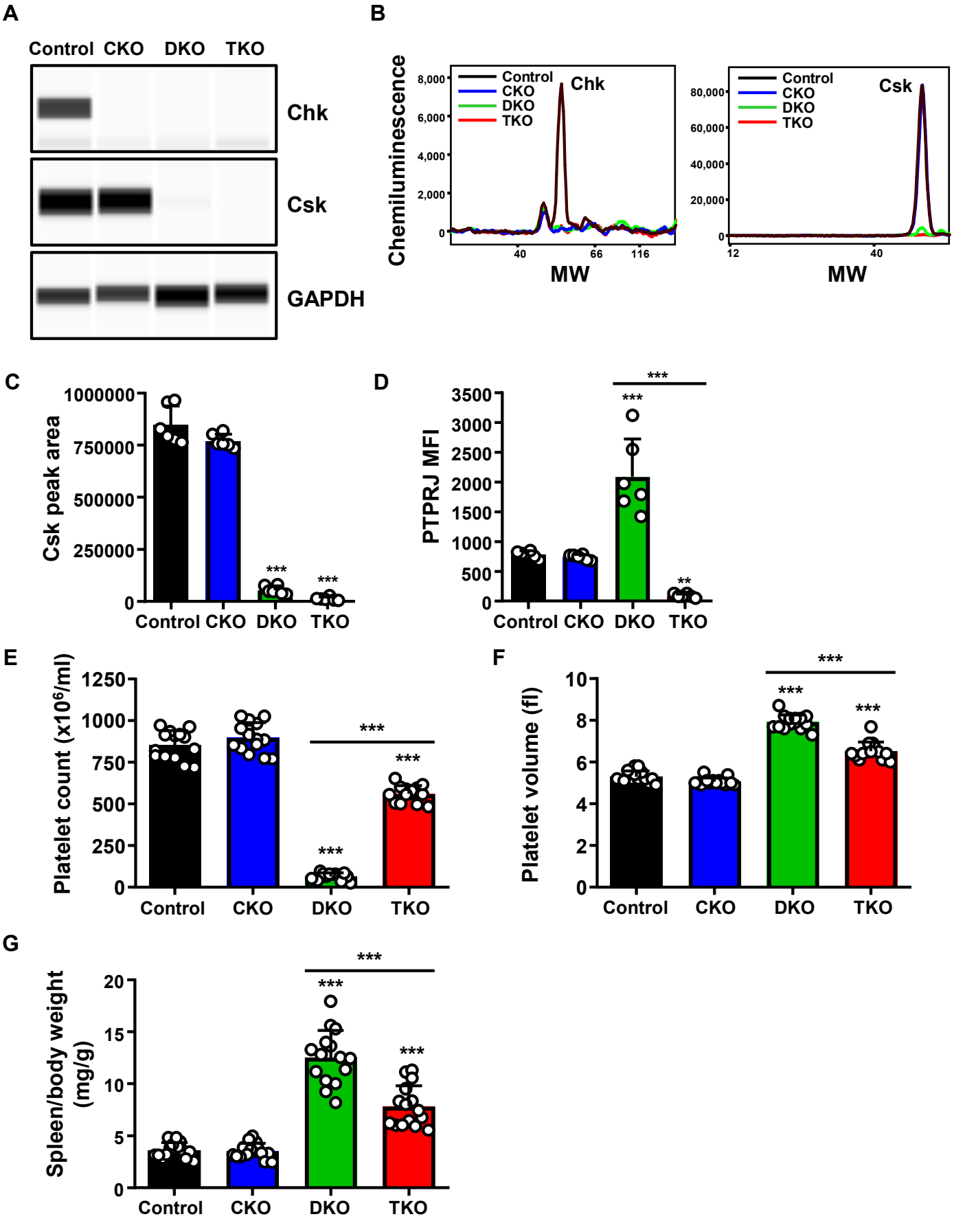
A
Control CKO DKO TKO
Chk
Csk
GAPDH
B
Chemiluminescence
Control
CKO
DKO
TKO
Chk
Csk
MW
C
Csk peak area
1000000
750000
500000
250000
0
***
Control CKO DKO TKO
D
PTPRJ MFI
3500
3000
2500
2000
1500
1000
500
0
***
**
Control CKO DKO TKO
E
Platelet count (x10^6/ml)
1250
1000
750
500
250
0
***
Control CKO DKO TKO
F
Platelet volume (fl)
10
8
6
4
2
0
***
Control CKO DKO TKO
G
Spleen/body weight (mg/g)
20
15
10
5
0
***
Control CKO DKO TKO

Figure 2

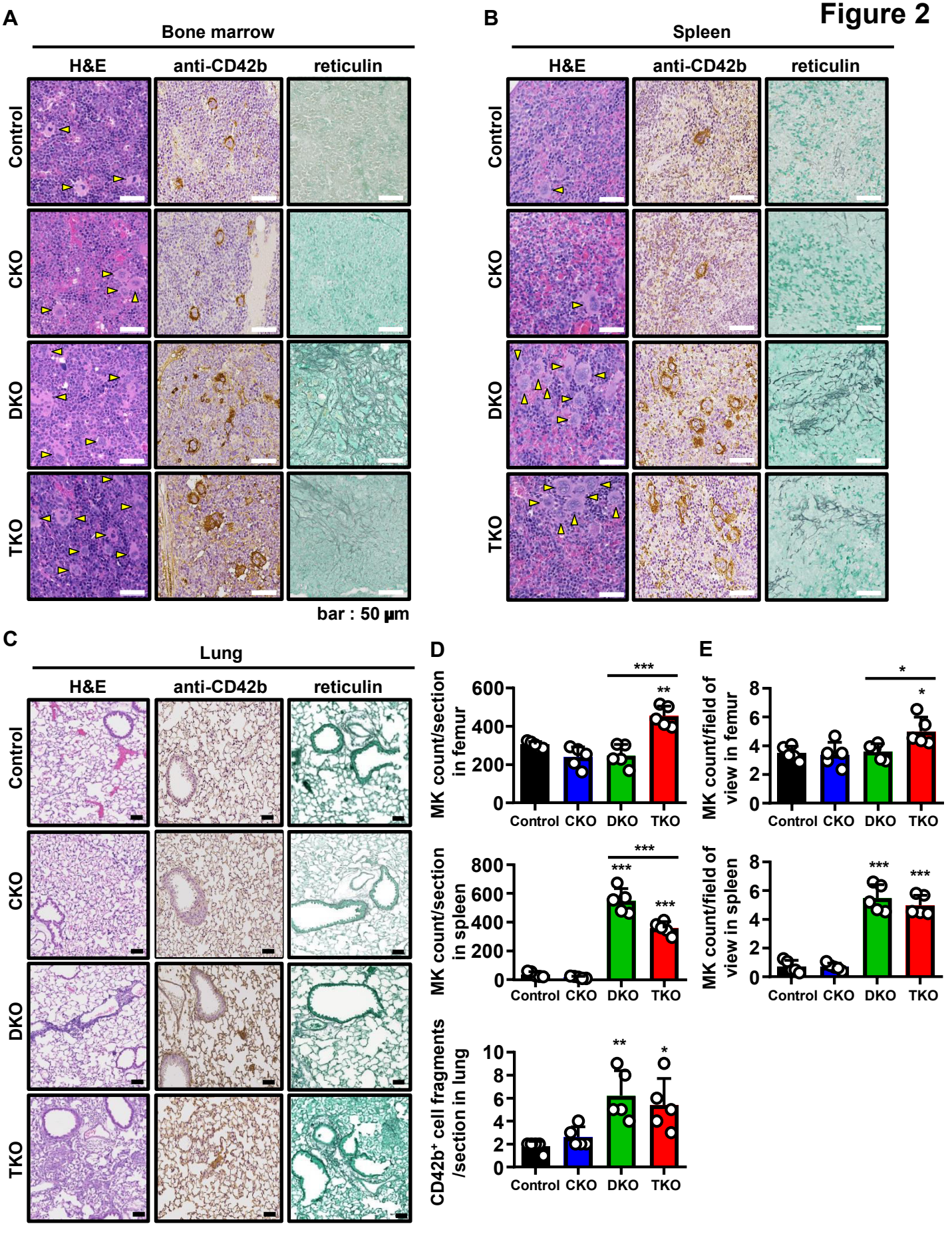
A
Bone marrow
H&E
anti-CD42b
reticulin
Control
CKO
DKO
TKO
bar : 50 μm
B
Spleen
H&E
anti-CD42b
reticulin
Control
CKO
DKO
TKO
C
Lung
H&E
anti-CD42b
reticulin
Control
CKO
DKO
TKO
D
MK count/section in femur
MK count/section in spleen
CD42b+ cell fragments /section in lung
Control
CKO
DKO
TKO
E
MK count/field of view in femur
MK count/field of view in spleen
Control
CKO
DKO
TKO

Figure 3

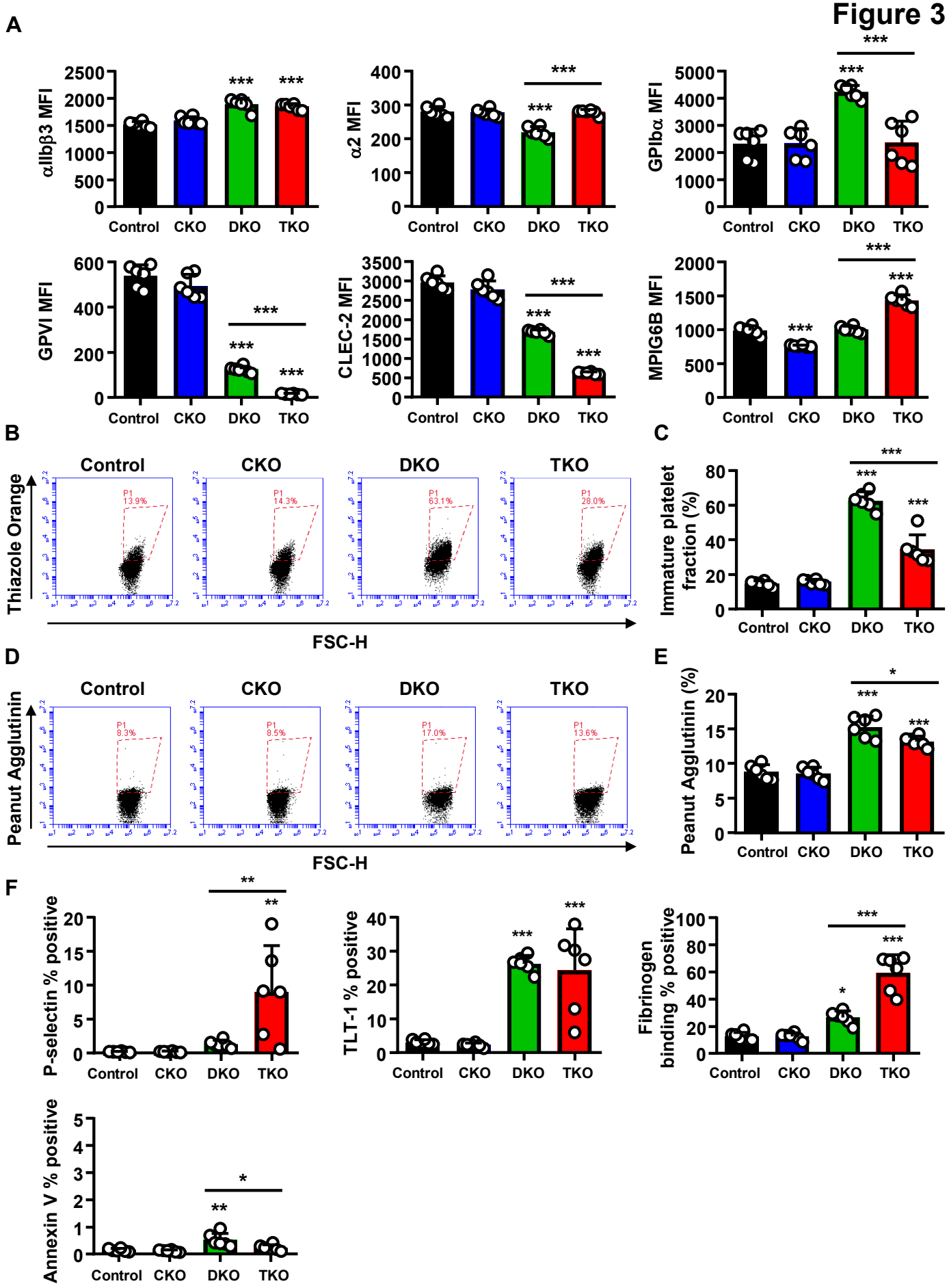
A
αIIbβ3 MFI
α2 MFI
GPIbα MFI
GPVI MFI
CLEC-2 MFI
MPIG6B MFI
Control
CKO
DKO
TKO
B
Thiazole Orange
FSC-H
P1
13.9%
14.3%
63.1%
28.0%
C
Immature platelet fraction (%)
D
Peanut Agglutinin
8.3%
8.5%
17.0%
13.6%
E
Peanut Agglutinin (%)
F
P-selectin % positive
TLT-1 % positive
Fibrinogen binding % positive
Annexin V % positive

Figure 4

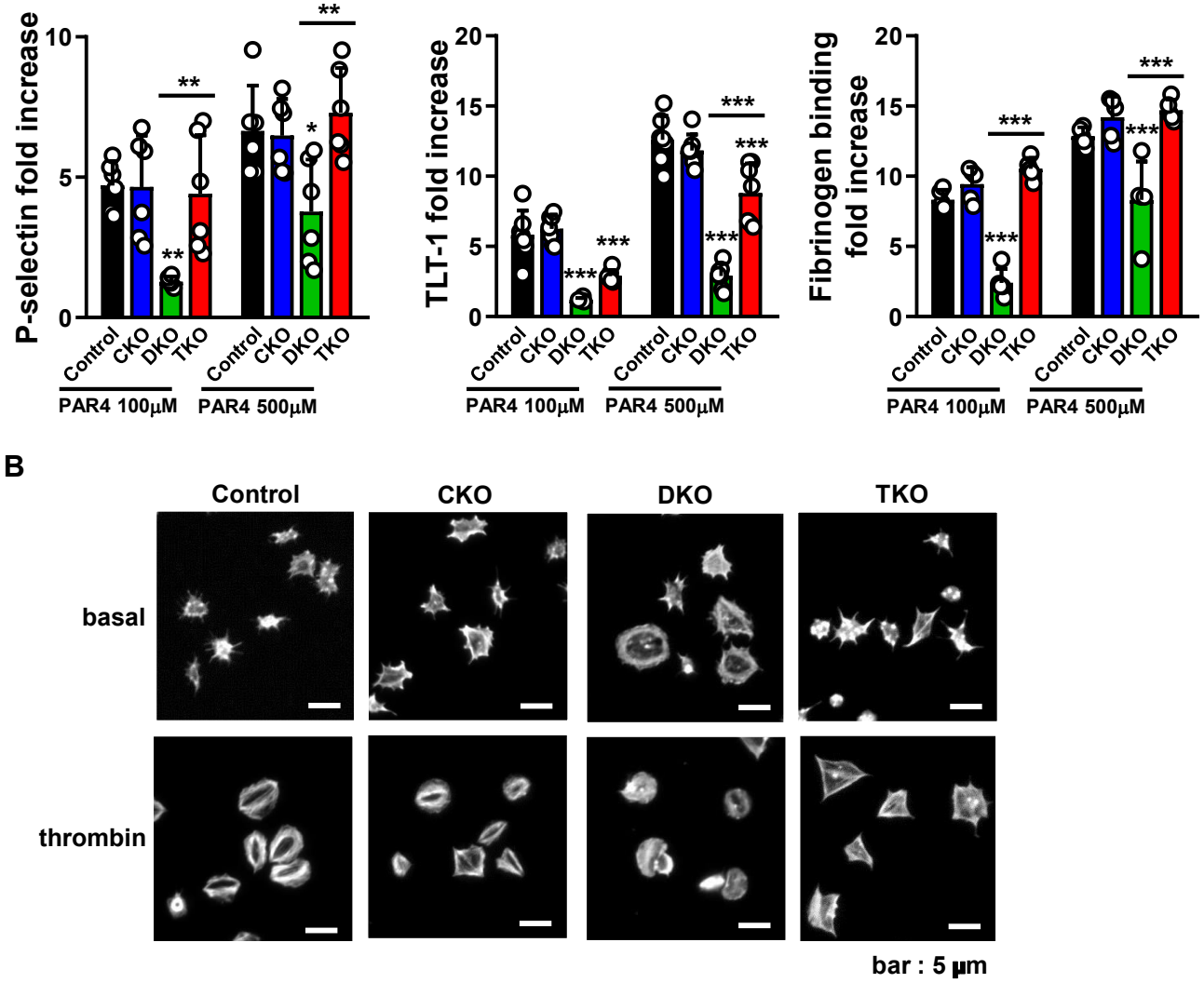
A
P-selectin fold increase
TLT-1 fold increase
Fibrinogen binding fold increase
Control
CKO
DKO
TKO
PAR4 100μM
PAR4 500μM
B
basal
thrombin
bar : 5 μm
C
Surface cover area (μm²)
basal
0.1 U/ml thrombin
100 μg/ml fibrinogen
D
Time (sec)

Figure 5

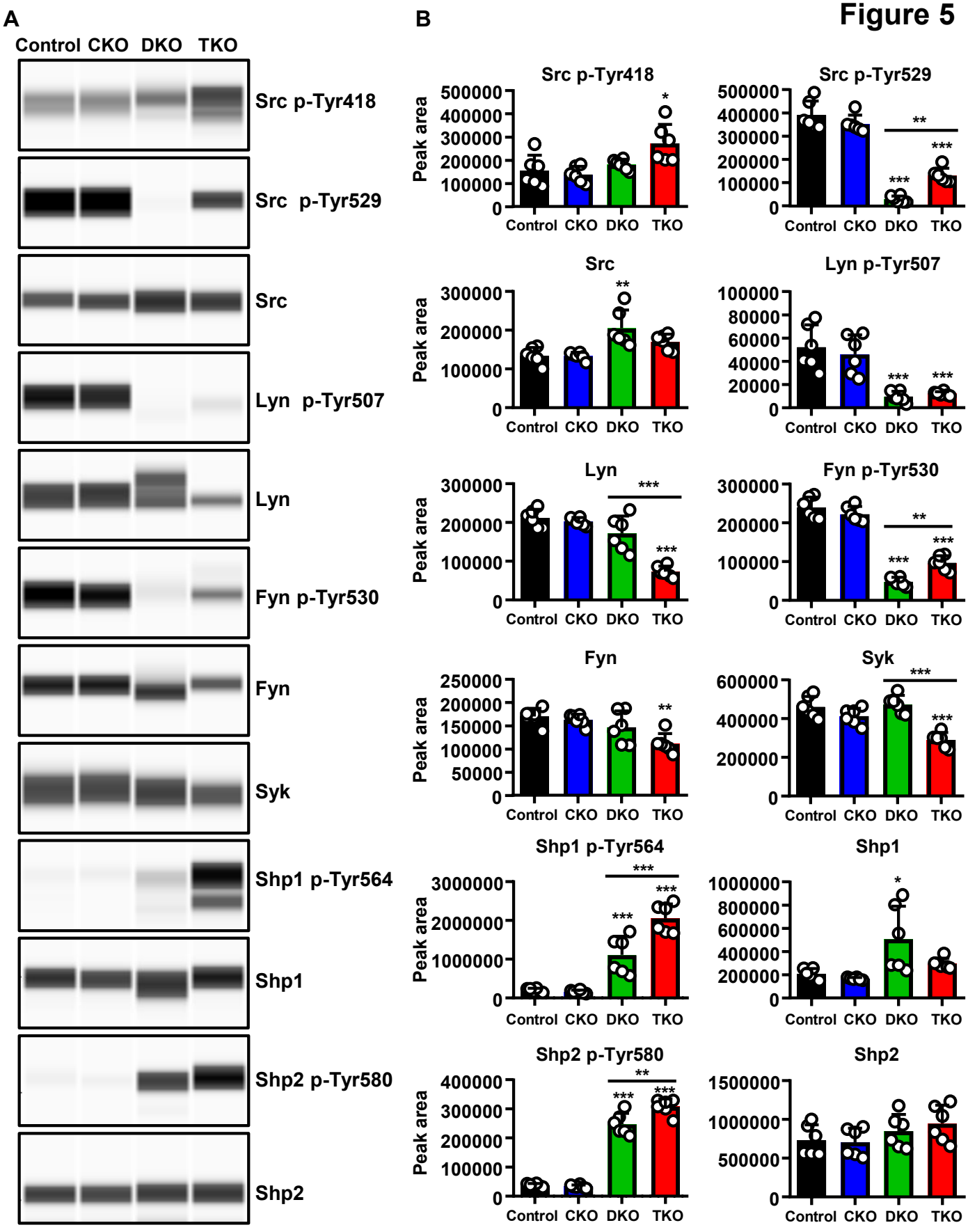
A
Control CKO DKO TKO
Src p-Tyr418
Src p-Tyr529
Src
Lyn p-Tyr507
Lyn
Fyn p-Tyr530
Fyn
Syk
Shp1 p-Tyr564
Shp1
Shp2 p-Tyr580
Shp2
B
Src p-Tyr418
Src p-Tyr529
Src
Lyn p-Tyr507
Lyn
Fyn p-Tyr530
Fyn
Syk
Shp1 p-Tyr564
Shp1
Shp2 p-Tyr580
Shp2
Peak area
Control CKO DKO TKO

Figure 6

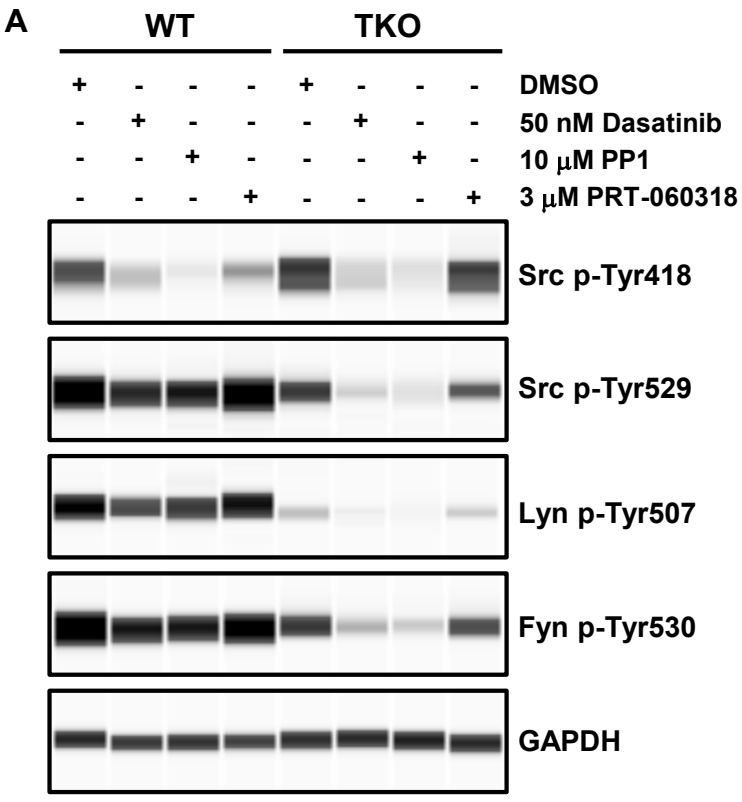
A
WT
TKO
+ - - - + - - - DMSO
- + - - - + - - 50 nM Dasatinib
- - + - - - + - 10 μM PP1
- - - + - - - + 3 μM PRT-060318
Src p-Tyr418
Src p-Tyr529
Lyn p-Tyr507
Fyn p-Tyr530
GAPDH

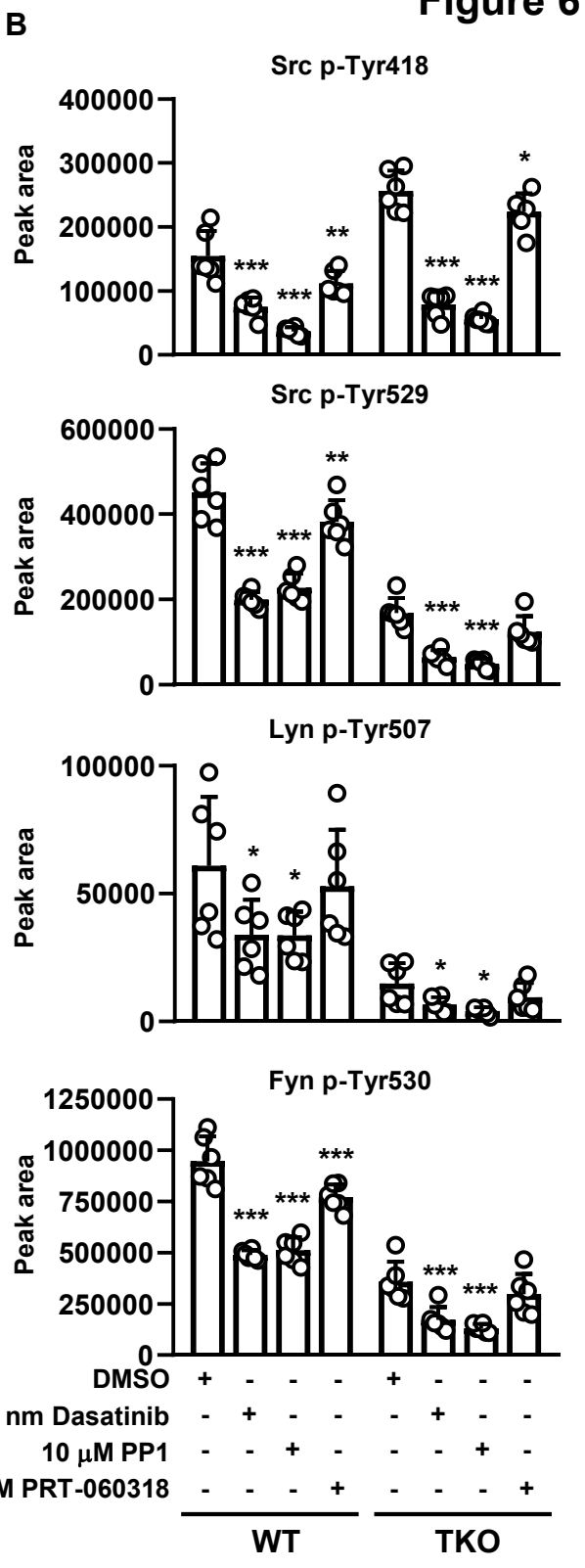
B
Src p-Tyr418
Peak area
400000
300000
200000
100000
0
Src p-Tyr529
600000
400000
200000
0
Lyn p-Tyr507
100000
50000
0
Fyn p-Tyr530
1250000
1000000
750000
500000
250000
0
DMSO + - - - + - - -
50 nm Dasatinib - + - - - + - -
10 μM PP1 - - + - - - + -
3 μM PRT-060318 - - - + - - - +
WT
TKO

Figure 7

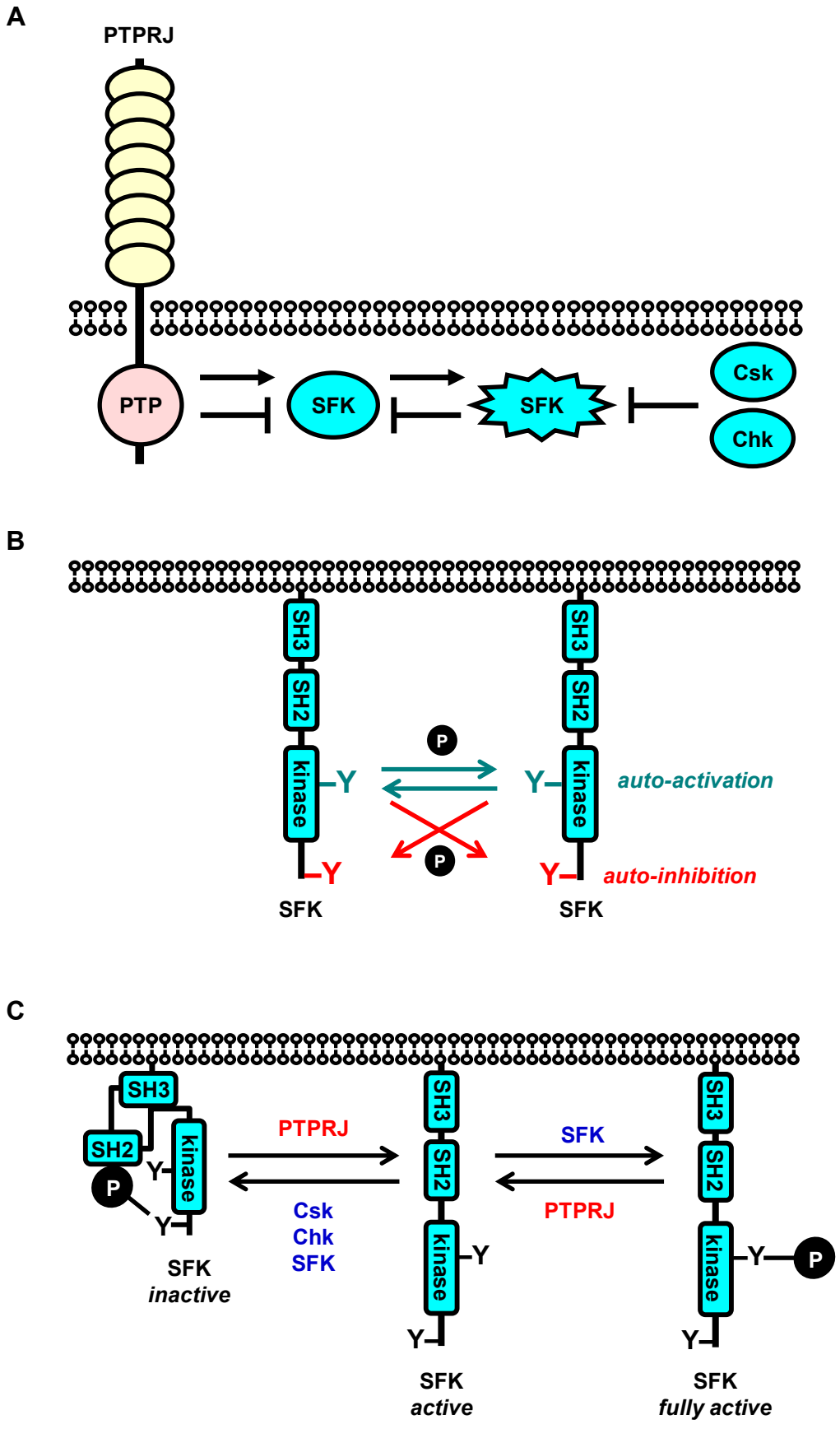
A
PTPRJ
PTP
SFK
SFK
Csk
Chk
B
SH3
SH2
kinase
Y
P
auto-activation
auto-inhibition
SFK
SFK
C
SH3
SH2
kinase
P
PTPRJ
Csk
Chk
SFK
SFK
inactive
SFK
PTPRJ
SFK
active
SFK
fully active

Supplemental Materials and Methods

Flow cytometry

Platelet surface glycoprotein expression or reticulated platelets were measured in whole blood using anti-αIIb and indicated antibodies as previously described.[1] Resting and PAR4 peptide (AYPGKF)-activated platelets were stained with FITC-conjugated P-selectin Ab, TLT-1 (Alexa Fluor 488) Ab or Alexa488-conjugated fibrinogen, and fixed with 1 % ice-cold formalin. Median fluorescence intensity (MFI) in αIIb positive cells or gated population in side scatter area (SSC) and forwards scatter (FSC) in 10,000 events was measured by flow cytometry (BD Biosciences Accuri C6).

Capillary electrophoresis-based immunoassays

For quantitative analysis, platelet whole cell lysates (WCLs) were analyzed with an automated capillary-based immunoassay platform (Wes, ProteinSimple, San Jose, USA), according to the manufacturer's instructions. Briefly, WCLs from resting platelets or platelets incubated with DMSO, 50 nM dasatinib, 10 μM PP1, or 3 μM PRT-060318 (for 15 min, at room temperature) were diluted to the required concentration with 0.1X sample buffer, then prepared by adding 5X master mix containing 200 mM dithiothreitol (DTT), 5X sample buffer and fluorescent standards (Standard Pack 1, PS-ST01-8) and boiled for 5 minutes at 95°C. Samples, antibody diluent 2, primary antibodies and anti-rabbit secondary antibody, luminol S-peroxide mix and wash buffer were displaced into Wes 12-230 kDa prefilled microplates, (pre-filled with separation matrix 2, stacking matrix 2, split running buffer 2 and matrix removal buffer, SM-W004). The microplate was centrifuged for 5 minutes at 2500 rpm at room temperature. To start the assays, the capillary cartridge was inserted into the cartridge holder and the microplate placed on the plate holder. To operate Wes and analyze results Compass Software for Simple Western was used (version 3.1.7, ProteinSimple). Separation time was set to 31 minutes, stacking loading time to 21 seconds and sample loading time to 9 seconds, and for detection the High Dynamic Range (HDR) profile was used. For each antibody, a lysate dilution experiment was performed first to confirm the optimal dynamic range of the corresponding protein on Wes. This was followed by an antibody optimization experiment to compare a range of dilutions and select an antibody concentration near to saturation level to allow a quantitative comparison of signals between samples. The optimized antibody dilutions and final lysate concentrations were as follows (antibody dilution, lysate concentration): Src p-Tyr418 (1:10,

0.05 mg/ml); Lyn p-Tyr507 (1:10, 0.32 mg/ml); Shp1 p-Tyr564 (1:10, 0.32 mg/ml); Shp1 (1:10, 0.2 mg/ml) and Shp2 p-Tyr580 (1:10, 0.05 mg/ml) were incubated for 60 minutes, whereas Src p-Tyr529 (1:100, 0.025 mg/ml); Fyn p-Tyr530 (1:50, 0.025 mg/ml); Src (1:50, 0.05 mg/ml); Lyn (1:25, 0.05 mg/ml); Fyn (1:25, 0.05 mg/ml); Syk (1:10, 0.00625 mg/ml); Shp2 (1:10, 0.00625 mg/ml); Csk (1:10, 0.05 mg/ml); Chk (1:80, 0.2 mg/ml); GAPDH (1:10, 0.05 mg/ml) were incubated for 30 minutes.

Immunohistochemistry

Femurs, spleens and inflated lungs were fixed in buffered formalin and embedded in paraffin. Sections were stained with haematoxylin and eosin (H&E), reticulin (Gordon & Sweet) or anti-CD42b antibody by Advance Histopathology Laboratory Ltd (London UK). Images were obtained by Slide Scanner Axio Scan.Z1 brightfield microscope (Zeiss) and microscope (Leica). MK count analysis in whole section and per field view was performed in a double blinded manner.

Static adhesion spreading assay

Washed platelets were pre-incubated with or without thrombin (0.1 Unit/ml, 5 minutes, room temperature) placed on fibrinogen-coated cover-slips as previously described.[1] Platelets were fixed with 4% formalin, permeabilised by 0.2% Triton X-100 and stained with Alex Fluor 488-phalloidin. Platelets were imaged by an Epi-fluorescence microscope (Zeiss) with an x63 oil immersion lens. A semi-automated machine learning based KNIME workflow was used to quantify the area of spread platelets as previously described.[2] Images were blinded before the quantification. An ilastik pixel classifier was used to produce a binary segmentation. To separate touching platelets, the centre of individual platelets were manually selected using KNIME. These coordinates were used to produce the final segmentation of individual platelets, and platelet size and shape were then calculated.

References

1. Mori J, Nagy Z, Di Nunzio G, et al. Maintenance of murine platelet homeostasis by the kinase Csk and phosphatase CD148. *Blood*. 2018;131(10):1122-1144.
2. Khan AO, Maclachlan A, Lowe GC, et al. High-throughput platelet spreading analysis: a tool for the diagnosis of platelet- based bleeding disorders. *Haematologica*. 2019.

Table S1

Hematological analysis of *Chk* KO, *Chk;Csk* DKO and *Chk;Csk;Ptprj* TKO mice.

Parameter	Control	CKO	DKO	TKO
PLT ($10^3/\mu L$)	853.1 ± 86.2	896.6 ± 89.6	64.4 ± 21.5***	560.3 ± 50.0***
MPV (fL)	5.3 ± 0.28	5.06 ± 0.18	7.91 ±0.35***	6.53 ±0.43***
RBC ($10^6/\mu L$)	9.22 ± 0.55	9.00 ± 0.50	7.88 ± 0.33***	8.46 ± 0.43***
HCT (%)	29.16 ± 1.6	27.83 ± 1.56	26.35 ± 1.46***	26.94 ± 1.36**
WBC ($10^3/\mu L$)	8.79 ± 2.66	7.63 ± 1.74	8.34 ± 1.95	7.68 ± 2.66
LYM ($10^3/\mu L$)	6.79 ± 1.92	5.99 ± 1.81	6.46 ± 1.55	5.87 ± 1.31
MON ($10^3/\mu L$)	0.38 ± 0.25	0.08 ± 0.04**	0.22 ± 0.09	0.32 ± 0.34
NEU ($10^3/\mu L$)	1.34 ± 0.6	0.53 ± 0.14***	0.57 ± 0.20***	0.76 ± 0.48**
BAS ($10^3/\mu L$)	0.009 ± 0.01	0.002 ± 0.01	0.009 ± 0.01	0.008 ± 0.01

PLT, platelets; MPV, mean platelet volume; RBC, red blood cells; HCT, haematocrit, WBC, white blood cells; LYM, lymphocytes; MON, monocytes; NEU, neutrophils; BAS, basophils; CKO, *Chk* KO
Mean ± standard deviation, n=14, *$P < 0.05$, **$P < 0.01$, ***$P < 0.001$, one-way ANOVA with Sidak's test

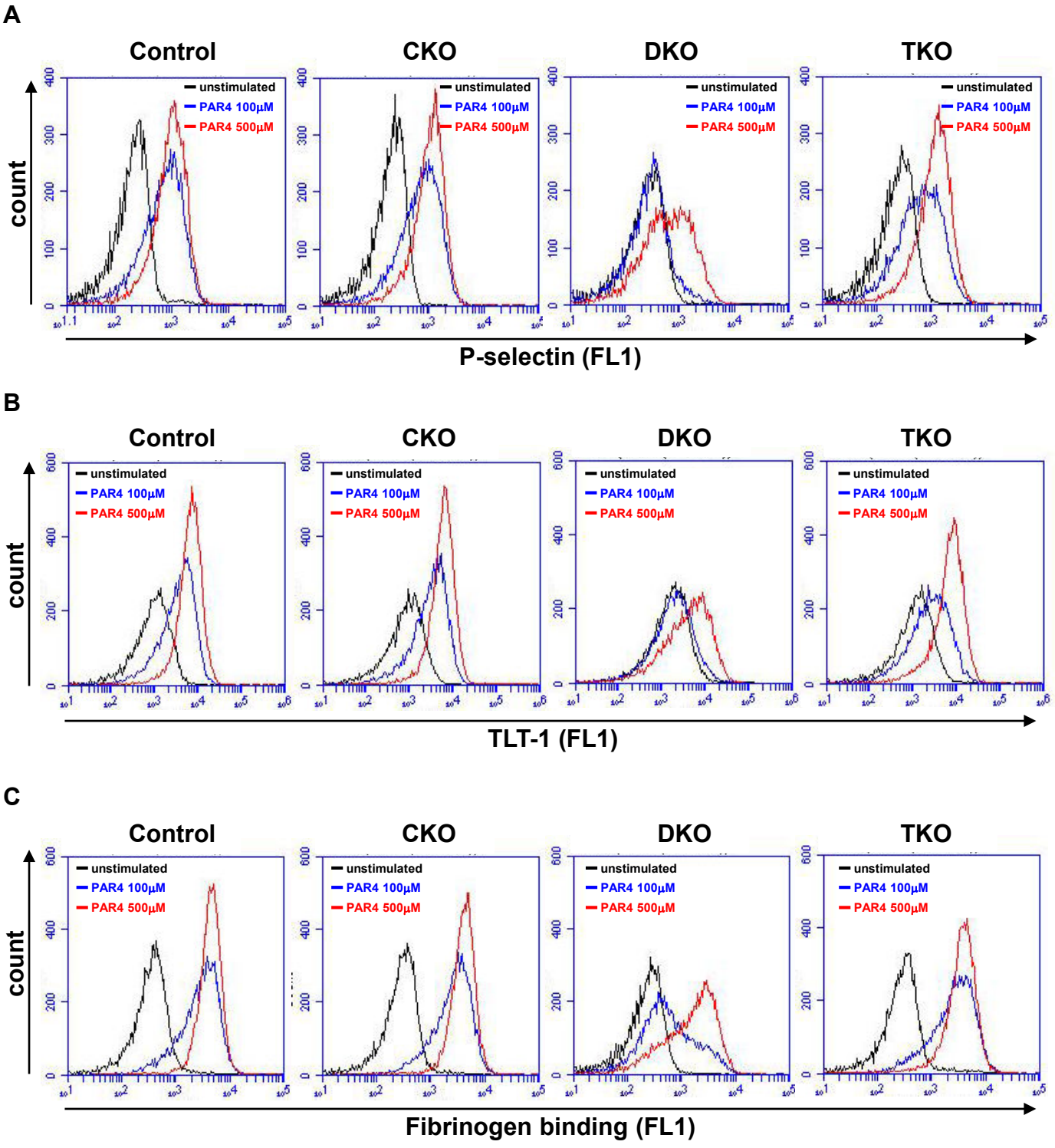

Figure S1. Defective platelet activation in DKO mice is restored in TKO mice. Representative plots (A) anti-P-selectin-FITC, (B) anti-TLT-1-FITC and (C) fibrinogen-488 binding to washed platelets (2 x 10^7/ml) which were either left unstimulated or following stimulation with PAR4 peptide (AYPGKF) (100 μM or 500 μM, 20 min, room temperature) as measured by flow cytometry.

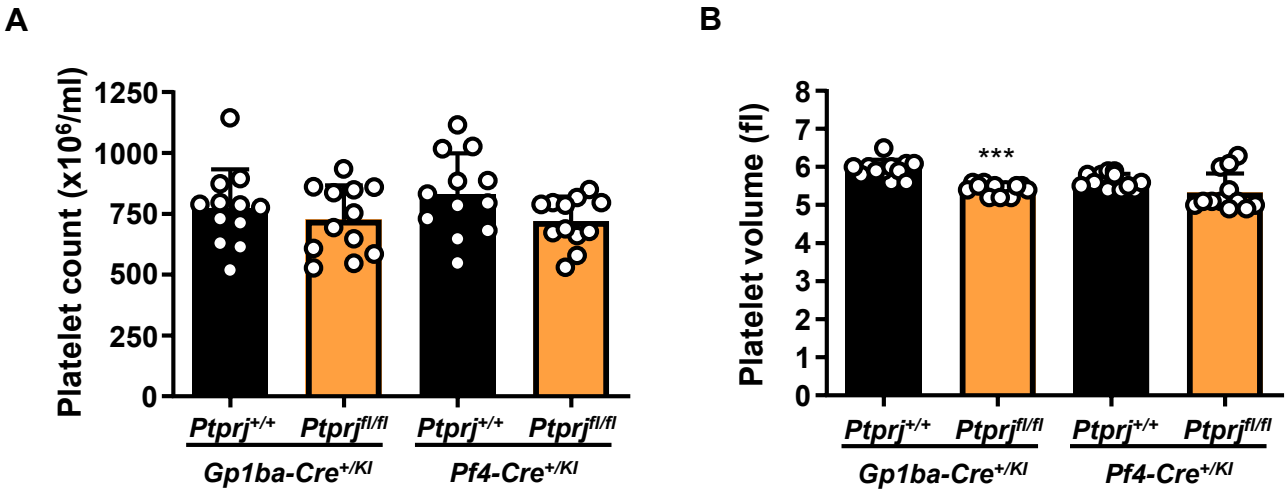

Figure S2. Normal platelet counts in *Gp1ba-Cre;Ptprj* and *Pf4-Cre;Ptprj* KO mice. (A) Platelet counts, n = 12 mice/genotype. (B) Platelet volumes, n = 12 mice/genotype. Asterisks refer to significant difference compared to respective controls. **P < 0.01, ***P < 0.001, one-way ANOVA with Sidak's test; mean ± SD.